

---

# An approach to synaptic learning for autonomous motor control

---

**Sergio Verduzco-Flores\***  
 Computational Neuroscience Unit  
 Okinawa Institute of Science and Technology  
 Okinawa, Japan  
 sergio.verduzco@gmail.com

**William Dorrell**  
 CNU, OIST  
 dorrellwec@gmail.com

**Erik DeSchutter**  
 CNU, OIST  
 erik@oist.jp

## Abstract

In the realm of motor control, artificial agents cannot match the performance of their biological counterparts. We thus explore a neural control architecture that is both biologically plausible, and capable of fully autonomous learning. The architecture consists of feedback controllers that learn to achieve a desired state by selecting the errors that should drive them. This selection happens through a family of differential Hebbian learning rules that, through interaction with the environment, can learn to control systems where the error responds monotonically to the control signal. We next show that in a more general case, neural reinforcement learning can be coupled with a feedback controller to reduce errors that arise non-monotonically from the control signal. The use of feedback control reduces the complexity of the reinforcement learning problem, because only a desired value must be learned, with the controller handling the details of how it is reached. This makes the function to be learned simpler, potentially allowing to learn more complex actions. We discuss how this approach could be extended to hierarchical architectures.

## 1 Introduction

Animals are masters at motor control, but it remains unclear how they achieve this. To advance the study of animal motor control the best strategy may be to mimic the way they learn. In particular:

- The agent learns as its body interacts in real time with the environment. Preferably a physical body, transmission delays, and response latencies should be considered.
- The controller uses nothing more than neurons.
- Learning rules use only information locally available at the postsynaptic neuron. Rather than relying on labelled data, learning takes advantage of correlation between signals, and reinforcement learning mechanisms.
- No element of the model goes against current consensus in neuroscience.

Models with these characteristics are rare. One reason is the significant challenge of performing motor control exclusively using neural elements. More than 70 years ago Cybernetics recognized

---

\*Corresponding Author.

the challenge of motor control in biological organisms [20], and emphasized the role of feedback control in an abstract way, without addressing the problem of neural implementations.

A more practical viewpoint was put forward by Perceptual Control Theory (PCT) [23]. The tenets of PCT can be stated in these (oversimplified) terms: through evolution the organism has an innate knowledge of the the perceptions which are conducive to homeostatic states. The organism is constantly attempting to create those perceptions, and this is what it learns through interaction with the environment. Matching desired and actual perceptions is a control problem, which PCT addresses using a hierarchy of feedback control systems. Although provocative, PCT research is yet to produce autonomous agents approaching state of the art. Despite steady progress in control theory for more than one century, it is still not feasible to create an autonomous agent by using feedback control to create desired values of homeostatic variables. We will outline why this is the case.

A feedback control system receives a vector of errors and outputs a vector of control signals. The *control law* maps errors to control signals so as to reduce the errors. This map is conventionally obtained by a designer using a model of the physical system to be controlled, called the *plant*. For example, the linear-quadratic regulator (LQR) is a feedback controller whose control law can be found by minimizing a quadratic cost function using either the Hamilton-Jacobi-Bellman equation, or Pontryagin's maximum principle [14].

Solutions such as the LQR are highly effective in particular situations, but they seem unsuited for specifying more general behaviours. Consider the case of an agent that must maintain regular levels of certain homeostatic variables, such as blood sugar, or nociceptors' activity. These variables are not directly controllable, as would be the case of limb position. Instead, the variables to be controlled must be set through interaction with the environment. Designing a controller for this case requires a model, not only of the agents body, but also of the environment, and how they interact. This quickly becomes untractable for conventional control theory approaches.

Using a control law that is not designed *a priori*, but instead is learned through interaction with the environment is the main concern of Reinforcement Learning (RL) [31]. This discipline has had notable success in controlling agents in limited environments, but it can quickly run into the curse of dimensionality as the space of possible policies grows. The use of deep networks in order to learn value functions and policies (called deep RL) can improve this, leading to human or beyond human performance in some game environments [18, 29, e.g.] Using more realistic bodies and environments remains a challenge.

In part inspired by the anatomical structure of animal brains, hierarchical architectures [16] hold the promise of taming the curse of dimensionality. Both hierarchical RL [2] and hierarchical deep RL [11] are areas of ongoing research, but it remains unclear how these approaches can best harness the learning and representational power of neural networks. Moreover, it is not known whether their computations parallel those in animal brains. This motivates the development of biologically-plausible models of hierarchical RL [24, 6, 19, 7].

We present a family of synaptic learning mechanisms allowing a feedback control system to adjust so as to reduce an arbitrary error, as long as the error and the motor commands have a monotonic relation. In other words, the motor command should not cause the error to increase in one context, and to decrease in a different one. We consider that for low levels of a control hierarchy, where the response properties of actuators must be learned and continuously adjusted, learning using correlations between signals is a better approach than using global rewards. Our learning mechanisms offer a novel approach to do this.

We illustrate how our learning rules can be used to control two simple systems. Next we show how the restriction of a monotonic relation between errors and motor commands in a feedback controller can be overcome using reinforcement learning to adjust the controller according to the current context.

In the Discussion we describe new results and future directions, including realistic simulations of 2D arm reaching, and a hierarchical version of an architecture presented in this paper.

## 2 Preliminaries

The feedback control problem we consider is depicted in figure 1A. The  $P$  block represents a plant that encapsulates both the agent’s body and the environment, which send *afferent* signals to a sensory population  $S_P$ , producing the perceived value of the state. A separate population  $S_D$  represents a desired value for the perceived state  $S_P$ . A controller  $C$  receives the activity of both  $S_D$  and  $S_P$ , mapping them into a motor command to the agent’s actuators.

A common configuration for feedback control is shown in panel B of figure 1. In here the input to the controller is an error consisting of the difference between the desired and the actual observation. In the case when  $S_D$  and  $S_P$  are scalar values a simple strategy such as Proportional-Derivative (PD) control [30] can be autonomously configured, and achieve acceptable performance. When  $S_D$ ,  $S_P$ , and the output of the controller are high-dimensional we say the system is Multi-Input Multi-Output (MIMO).

MIMO systems present a particular set of challenges, and control theory has a well-developed array of techniques to overcome them (e.g. [13]). Most of those techniques assume a mathematical model of the plant, which, as we have discussed, is not feasible in our case. Among those techniques that do not assume a model of the plant (e.g. data-driven control systems), very few use biologically realistic neural networks in their solution.

Four control architectures using biologically-plausible neural networks have been identified [26]. From these, direct inverse learning [12] is an offline method, whereas distal supervised learning [9], and feedback error learning [17] rely on backpropagation in order to train forward and/or inverse models of the plant.

The fourth architecture is Reinforcement Learning, which avoids the limitations of the other architectures, but is generally slower to find a solution. Given the close ties between RL and differential Hebbian learning [10], it is interesting to ask whether the correlations between inputs and outputs to the controller can be used to obtain a control law that is adaptive and biologically plausible as RL, but can achieve faster learning.

## 3 Results

### 3.1 Learning rules for online adaptive control

Looking at the population  $C$  in panel B of figure 1, we can see that if we had a module that *cancels its own inputs* this could provide a solution to the neural control problem. The actions of this module would also promote stability of this recurrent network. To create such a device we follow this intuition: if one of  $C$ ’s outputs controls one of its inputs, then that input will resemble a slightly delayed version of that output (with a possible sign reversal, as the action can increase or decrease the error). If we can measure this resemblance in a way that is somewhat invariant to scaling, mean values, and small difference in the phases, then we can configure the weights of a negative feedback controller capable of reducing that input.

Assume that the error is an  $M$ -dimensional vector  $\mathbf{e} = [e_1, \dots, e_M]$ , and that  $C$  contains  $N$  units, whose activity is in the vector  $\mathbf{c} = [c_1, \dots, c_N]$ . If there are lateral connections among the  $C$  units, then they can have the  $c_k$  values locally available. The synaptic weight  $\omega_{ij}$  for the connection from  $e_j$  to  $c_i$  will then have a time derivative:

$$\dot{\omega}_{ij}(t) = \Gamma_{ij}(\mathbf{c}(t - \Delta t), \mathbf{e}(t)),$$

where  $\Gamma_{ij}$  is a differential operator. We consider a family of Hebbian-like learning rules where:

$$\Gamma_{ij}(t) = -\alpha G_j(\mathbf{e}(t)) H_i(\mathbf{c}(t - \Delta t)) \quad (1)$$

where  $\alpha$  is a learning rate, and  $G_j, H_i$  are differential operators. In the rest of this subsection we will derive three equations of this type, whose performance will be tested later in the paper.

In the simplest interpretation  $G_j$  measures the activity of  $e_j$ , whereas  $H_i$  measures the activity of  $c_i(t - \Delta t)$ .  $G_j = e_j(t)$ ,  $H_i = c_i(t - \Delta t)$  produces Hebbian learning with a time delay. This rule, however, is not invariant to scaling or mean values, and the weights will tend to saturate. A more attractive choice is to use the correlation of the first derivatives. This provides a measure of whether

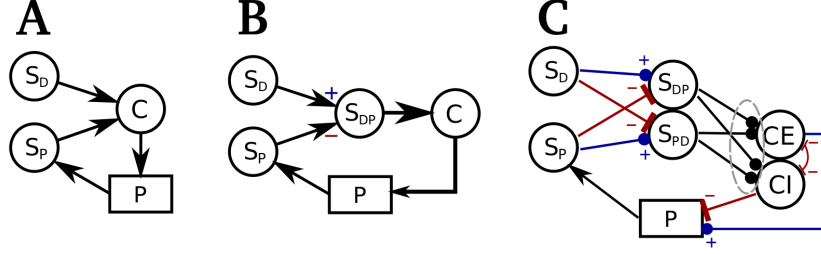


Figure 1: Basic feedback control architectures. All the modules depicted by a circle represent populations of neural units whose output is a scalar value between 0 and 1 (e.g. firing rate neurons). A) A general setup; the goal is to produce the same value in  $S_P$  and  $S_D$ . B) Negative feedback control. C) Negative feedback control with dual populations, as described in section 3.2. Connections inside the gray dashed oval are adjusted using the rules of section 3.1.

$c_i$  and  $e_j$  change together, in a way that is invariant to their mean values. The resulting learning rule is:  $\dot{\omega}_{ij}(t) = -\alpha \dot{e}_j(t) \dot{c}_i(t - \Delta t)$ .

The differential rule above can be improved by noticing that changes in  $e_j(t)$  could coincide temporally with those of  $c_i(t - \Delta t)$ , but the main cause of those changes may in fact be a different output  $c_k$ . It may thus be beneficial to introduce some competition among the synapses, as in:

$$\dot{\omega}_{ij}(t) = -\alpha \left( \dot{e}_j(t) - \langle \dot{e}(t) \rangle \right) \left( \dot{c}_i(t - \Delta t) - \langle \dot{c}(t - \Delta t) \rangle \right) \quad (2)$$

where  $\langle \dot{e} \rangle \equiv \frac{1}{M} \sum_k \dot{e}_k$ , and  $\langle \dot{c} \rangle \equiv \frac{1}{N} \sum_k \dot{c}_k$ . This rule bears some resemblance to the relative gain array criterion [3], which measures interactions in decentralized control systems. This is explained in the Appendix.

The dependence of  $\mathbf{e}$  on  $\mathbf{c}$  may take the form  $D\mathbf{e} = F(\mathbf{c})$ , where  $D$  is a differential operator, and  $F$  a vector function. This implies that the correlations may appear in mixed order derivatives, as would be the case between force and displacement in a system following Newton's laws. We illustrate this with:

$$\dot{\omega}_{ij}(t) = -\alpha \left( \ddot{e}_j(t) - \langle \ddot{e}(t) \rangle \right) \left( \dot{c}_i(t - \Delta t) - \langle \dot{c}(t - \Delta t) \rangle \right) \quad (3)$$

We may also introduce dependency on the errors in the  $H_i$  term of equation 1. One case comes from introducing a "global" error  $\|\mathbf{e}(t)\| = \sum_k e_k(t)$ . In the architecture of section 3.2 (Fig.1C), the  $e_k$  values are non-negative, so the sum of elements is the  $L^0$  norm. We now interpret  $G_j$  as a measure of how active  $e_j(t)$  was compared with all the other  $e_k$  values, whereas  $H_i$  measures how much  $c_i(t - \Delta t)$  contributes to  $\|\mathbf{e}\|$  using correlations among derivatives. An example of such a rule is:

$$\dot{\omega}_{ij}(t) = -\alpha \left( [\dot{e}_j(t) - \langle \dot{e}(t) \rangle] [ \|\dot{\mathbf{e}}(t)\| \dot{c}_i(t - \Delta t) + \|\ddot{\mathbf{e}}(t)\| \ddot{c}_i(t - \Delta t) ] - \dot{\Lambda}(t) \dot{c}_i(t) \right) \quad (4)$$

where  $\Lambda$  is the scaled sum of inputs from  $C$ , namely  $\Lambda = \sum_k w_{ik} c_k$ . The  $\dot{\Lambda}(t) \dot{c}_i(t)$  term is useful to desynchronize  $C$  units that inhibit each other, so they don't potentiate the same inputs. A motivation for using higher order derivatives in this rule is that similarity between  $\mathbf{e}(t)$  and  $c_i(t - \Delta t)$  will reflect in similar Taylor expansions.

A different approach is to let  $H_j$  be an integral operator that measures the similarity between the power spectra of the error and command signals, which is invariant to phase differences. Due to its non trivial neural implementation this is not pursued in this paper.

As can be surmised, other rules can be devised. We limit ourselves to exploring equations 2, 3, and 4.

### 3.2 An architecture for monotonic online adaptive control

In order to test learning rules like equations 2, 3, and 4 we created a more biological version of the architecture in panel B of figure 1. This is depicted in panel C.

Since we interpret our units as firing rate neurons, we don't consider any negative activities other than possibly the plant. To handle positive and negative errors we use two populations,  $S_{DP}$ , and  $S_{PD}$ .  $S_{DP}$  receives excitation from  $S_D$ , and inhibition from  $S_P$  (which would come from feed-forward inhibition, not explicitly modelled). Inhibition and excitation are swapped in  $S_{PD}$ , so that together with  $S_{DP}$  these populations create a dual representation where the magnitude of the error increases the activity, regardless of its sign.

The  $C$  population maintains this duality, as it is divided into  $CE$  and  $CI$  components. Each unit in  $CE$  has a counterpart in  $CI$ , and they mutually inhibit one another, reflecting the organization of motor units in agonist-antagonist pairs, as commonly found in vertebrates.

It can be shown that using linear units and a learning rule as in equation 2 in the Fig.1B network allows convergence to fixed points with non-zero error (see Appendix). To avoid this we use a specialized type of unit inspired by intrinsic oscillators in the spinal cord [15]. The response of each unit in  $CE$  and  $CI$  consists of two parts. One is the integral of its inputs, and the other is a sinusoidal (or a rectified sinusoidal) whose amplitude is modulated by the input. The specific equations can be found in the appendix. The rest of the units are sigmoidals, except for those in  $S_D$ , whose activity is a fixed function of time. Projections from  $P$  to  $S_P$  were one-to-one with unit weights. The weights of connections from  $S_{PD}/S_{DP}$  undergo divisive normalization [4] so that their sum remains constant.

### 3.3 Simulations of simple monotonic control

We simulated each of the learning rules in equations 2, 3, and 4 for two simple models of the plant  $P$ . The learning rules depend on the relative timing of the error and command signals. To properly test them we need to consider transmission delays and latencies in the response of the units, which may be significant in biological organisms. For this purpose we use the Draculab simulation software [32]. Each unit and synapse is modeled with an ordinary differential equation, and transmission delays are considered.

In the first model each unit  $c_j^e$  in  $CE$  was associated with a vector  $\mathbf{v}_j$ , whereas the corresponding unit  $c_j^i$  in  $CI$  was associated with  $-\mathbf{v}_j$ . The output of the plant was a vector  $\mathbf{p}$  defined as  $\mathbf{p} = \sum_j (c_j^e - c_j^i) \mathbf{v}_j$ , where  $c_j^e, c_j^i$  are also used to denote the activity of those units. The task of the network in this case is akin to solving a linear system. For a given desired vector  $\mathbf{s}_D$  in  $S_D$ , there is a vector  $\mathbf{p}_D$  that makes the activity in  $S_P$  match  $\mathbf{s}_D$ . The network must find a weight matrix  $W_{CP}$  from  $C$  to  $P$ , and a vector  $\mathbf{c}$  of activities in  $C$  such that  $\mathbf{p}_D = W_{CP} \mathbf{c}$ .

This problem can only be solved when  $W_{CP}$  has full rank. Moreover, as would be expected from a decentralized control system, as the interaction between the controlled variables increases the problem becomes more difficult, and performance begins to decrease [13, Ch.74]. This means that increasing the number of columns with similar non-zero elements will cause interactions among the controllers, which may be reflected as a larger error.

To explore this we selected four types of  $\mathbf{v}_j$  vectors. For the first type, the matrix with the  $\mathbf{v}_j$  vectors for columns was the identity matrix. In the second type the  $\mathbf{v}_j$  vectors constituted a Haar basis, which is an orthogonal basis with 1 and  $-1$  entries; in this case the activity of any  $C$  unit will affect all errors. In the third type the set of  $\mathbf{v}_j$  vectors was the union of the sets from the two previous cases, creating an overcomplete basis in the  $W_{CP}$  matrix. For the final type all  $\mathbf{v}_j$  vectors were random, and there were 3 for each unit in  $S_P$ . Simulations were run for 1, 2, 4, and 8 units in  $S_P$ . Results are summarized in figure 2. The third and fourth types of connectivity are respectively labeled *overcomplete*, and *overcomplete2* in this figure.

It can be seen that tracking one or a few values is easy for any of the rules, but higher dimensionality of  $S_P$ , and a high degree of interaction between its components makes the task more difficult. The effect of redundancy in the actuators (overcomplete  $W_{CP}$ ) is less marked.

The second plant model is a pendulum that stops when trying to rotate across a certain angle, so monotonic control is maintained.  $C$  uses two units, one providing clockwise, and another counter-clockwise torque. The value in  $S_D$  represents a given angle, and the task is to move the pendulum to that angle so activity in  $S_P$  and  $S_D$  can be equal.

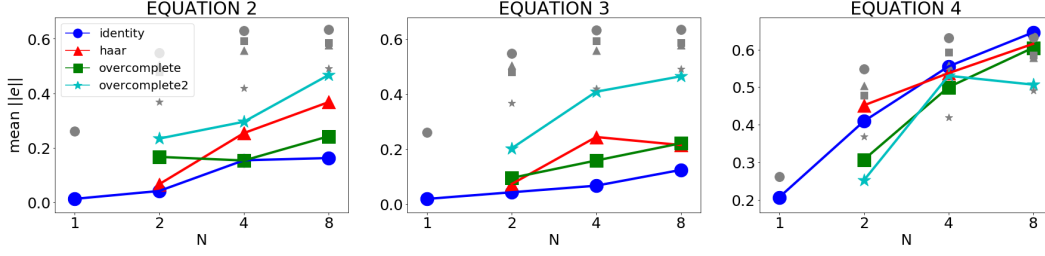


Figure 2: Simulation results for 4 types of connectivity matrices in a linear plant model. The number of values in  $S_P$  is labelled  $N$  in the x-axis. The y-axis indicates the time average of the norm  $\|s_P - s_D\|$  for the second half of the simulation, where  $s_P$  is the vector of activities in  $S_P$ , normalized so it has a unit norm for  $N > 1$ , and likewise for  $s_D$ . Gray markers indicate the same mean error when a simulation with the same characteristics was run with static synapses. In the case  $N = 1$  only the identity matrix is tested.

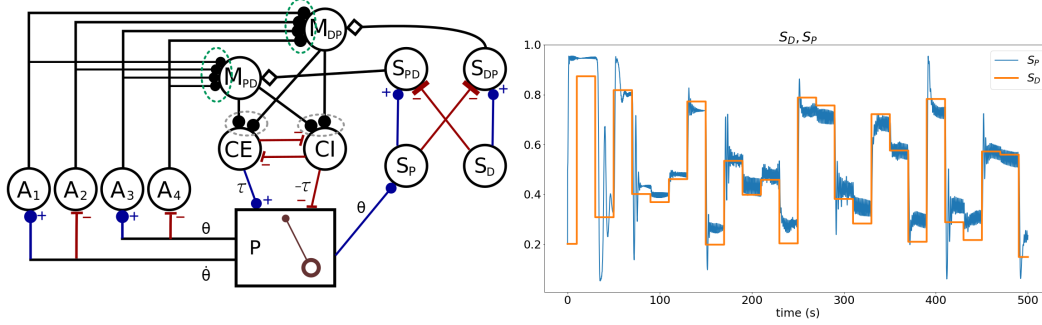


Figure 3: Pendulum tracking a desired angle. Left: Controller architecture. Each circle represents a single neuron, whereas the square represents the plant  $P$ . Blue connections are excitatory, red ones are inhibitory.  $\theta$  represents the current angle in radians, whereas  $\dot{\theta}$  is the angular velocity. These state variables are transformed into activation in the  $(0, 1)$  range by sigmoidal units in the  $A$  population. Both units in the  $M$  population receive all  $A$  signals. The connections from  $A$  to  $M$  (green dotted ovals) evolve following the input correlation rule, and the connections from  $M$  to  $C$  units (gray dotted ovals) evolve using the rule from equation 2. The output of the  $C$  units is mapped into either a positive or a negative torque ( $\tau$ ). Right: Activity of  $S_D$  (yellow), and  $S_P$  throughout a simulation. The effect of intrinsic 4 Hz oscillations in the  $C$  units can be observed in the  $S_P$  activity.

For this particular task the architecture of Fig.1C was extended with a population  $M$  receiving the *afferent* activity  $A$ , which consisted of the two pendulum state variables (the angle  $\theta$ , the angular velocity  $\dot{\theta}$ ) in their non-negative (dual) representation, resulting in four inputs (figure 3). The gain of each  $M$  unit was modulated by one of the two errors, either  $s_{DP}$ , or  $s_{PD}$ . The  $M$  units used the *input correlation* rule [22] to potentiate afferent inputs that correlate with the error that modulates them. This allows  $M$  to send  $C$  an error composed of afferent signals, resulting in a self-configuring proportional-derivative controller.<sup>2</sup> This scheme is inspired by the long reflex-loop, consisting signals that go from afferents to motor cortex, and from motor cortex to motoneurons.

Figure 3 shows a representative result, where the system learns to perceive a desired  $S_D$  angle in  $S_P$ . Full equations, and simulation details can be found in the Appendix.

<sup>2</sup>The  $C$  units in this version of the model output the integral of their input, so this is in fact a rather non-standard PI controller. For the model mentioned in section 4.1 these integrators are replaced by a pair of sigmoidal units, similar to the classic Wilson-Cowan model [5].

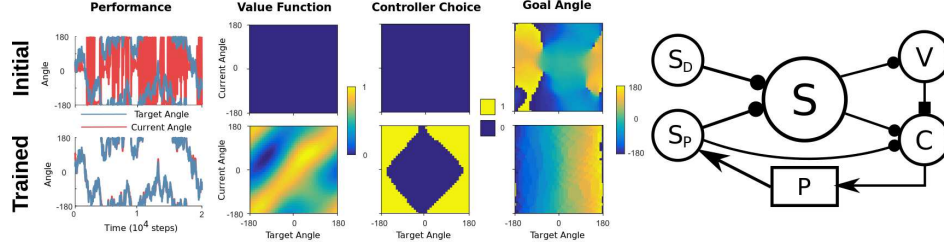


Figure 4: Actor-critic architecture used in section 3.4. Left: results of a representative simulation. Right: Connectivity diagram. See text for details.

### 3.4 An architecture for non-monotonic online adaptive control

Because the  $G_j, H_i$  terms in the learning rules of equations 2, 3, 4 are monotonic functions,  $c_i$  causing either positive or negative  $e_j$  errors depending on the context will create inconsistent correlations, making the approach unlikely to succeed.

A further complication is that the representation of sensory signals may not always be germane for negative feedback control. Muscle afferents use a firing rate code that provides information about the muscle's length, speed, and tension, but other afferents may provide a distributed representation, using a population of neurons where each one is tuned to a particular range of values (e.g. direction tuning in somatosensory cortex [21], or retinotopic location tuning in posterior parietal cortex [1]).

If a system such as ours is to be found at the bottom of a hierarchical system to control homeostatic variables, it should deal with the issues above. We have identified an actor-critic architecture that offers a plausible solution (figure 4, right). The actor  $C$  consists of one or more feedback controllers, each of which learns a to associate each state with a target value, and a configuration. The *state* network  $S$  does an expansive recoding of the activities in the  $S_D$ , and  $S_P$  populations (as in [8]) that permits the  $V$  and  $C$  networks to learn functions of the state using a single layer.  $V$  consists of a single unit that learns a value associated with each activity vector in  $S$ , using a neural version of the temporal differences algorithm. The value produced by  $V$  is in turn used so the actor  $C$  can learn a good controller configuration associated with each state. Notice that inclusion of  $S_D$  in the state representation allows for a natural way to produce a value function that is also dependent on the goal [27].

To make this concrete we implemented this architecture to solve the pendulum control problem as in the previous section, but in this case the pendulum is allowed to rotate freely. Given a desired angle  $\theta_D$ , and a current angle  $\theta$ , this problem cannot be solved efficiently by a controller that responds proportionally to  $\theta_D - \theta$ , because  $\theta$  is periodic (359 degrees and 1 degree are very close). The proportional controller does not cross the angle discontinuity, even if this is the shortest path to reach the desired angle.

In order to solve this problem we can have two angle representations for the controller, each possessing a discontinuity in a different region of the input space, in this case 0 and 180 degrees. For each state the network learns which of these afferent inputs to use, and also what  $\theta_D$  angle it should aim towards. The  $\theta_D$  angle is learned (e.g. it is not directly set from  $S_D$  into  $C$ ) so distributed afferent representations can be handled; this amounts to performing a coordinate transformation. This will become significant in section 4.2.

Learning the angle representation and the desired angle greatly benefits from having a value associated with each state, providing a measure of distance between  $S_D$  and  $S_P$ . This can be obtained using standard RL methods, although modified to work with this neural network in real time. Let  $\theta_D^*$  be the angle where  $s_P = s_D$ , whereas  $\theta_D$  denotes the target value of the controller. When  $\theta \approx \theta_D^*$  the system will experience a reward, used in a modified version of the neural TD learning rule [28] for the connections from  $S$  to  $V$ . The value that  $V$  outputs approximate conflates two factors: the time that the controller requires to bring  $\theta$  into  $\theta_D$ , and the time it takes to go from  $\theta_D$  into  $\theta_D^*$ .

The value from  $V$  can be used to train the connections from  $S$  to  $C$  so they choose the appropriate target value  $\theta_D$  given the current context. To this end we use a form of reward-modulated Hebbian learning, where the value from  $V$  is used for modulation. Full equations are in the Appendix.

Figure 4 shows representative results from a simulation of our actor-critic architecture. The system effectively learns to track a desired angle that changes through time in a noisy fashion. It should be observed that: 1) the final value function resembles the identity matrix, reflecting the fact that reward happens when  $s_P = s_D$ ; 2) the system learns to choose the afferent representation (“Controller Choice” in the figure) whose discontinuity is not in the shortest path between  $\theta$  and  $\theta_D$ ; 3) the system learns to set  $\theta_D \approx \theta_D^*$ , regardless of  $\theta$ , which is optimal in the case of our value function. Removing dependency on  $\theta$  in the policy is akin to reducing the dimensionality of the problem, which is possible thanks to the feedback controller in  $C$ .

An important challenge in the implementation of our architecture is that the three types of learning (learning the value, desired angle, and angle representation) must be decoupled. Our informal observations are that concurrent learning of angle representation and desired angle may interfere with each other. In order to decouple learning we thus had a training period where random target angles were given to the controller, allowing the system to learn both the value function and the best angle representation for each state. After this the policy (e.g. target angle for each state) could be easily learned. Although it required two phases, the difficulty of training and final performance of this model was similar to training an actor-critic architecture where the policy simply consisted of choosing negative or positive torques (see Appendix).

## 4 Discussion

### 4.1 A more realistic reaching simulation

Using the ideas presented here we extended the architecture of figure 3 for the task of planar arm reaching. The plant includes full double pendulum dynamics, with six Hill-type muscles providing redundant actuation. Each muscle provides 3 signals arising from models of the Ia, Ib, and II muscle afferents. These respond non-linearly, and in the case of the Ia afferent the response can briefly be nonmonotonic. All connections include transmission delays; unit and afferent activities come from differential equations presenting response latencies. The model receives desired values for the Ia and II afferent signals, and can autonomously learn how to produce them. To our knowledge no biologically-plausible model has managed to do this before, using only neurons.

Due to the model’s complexity, and to its potential biological insights, the full description of this work is presented in a separate paper (in preparation).

### 4.2 A hierarchy of controllers

The architecture illustrated in figure 4 has one important characteristic:  $C$  is a feedback controller controlling  $\theta$ , embedded within a feedback controller controlling  $s_P$ . Nothing stops us from replacing the negative feedback controller in  $C$  with a more general feedback controller of the type depicted in figure 4, so that the action of the high level controller is to set the target value of the lower level controller. Notice that the coordinate transformation done in the model of section 3.4 to find a target angle is, in this general setting, a process of subgoal selection. By generating rewards for a lower level when a “ $s_P = s_D$ ” event occurs at the next level we can construct a hierarchical neural reinforcement learning system, potentially capable of handling more complex tasks. In fact, the architecture of figure 4 is an adapted version of a biologically-inspired hierarchical architecture whose publication is under preparation (in a paper distinct from that mentioned in section 4.1).

### 4.3 Exploration and learning

The models in sections 3.3, and 3.4 present different solutions to the exploration vs. exploitation dilemma. The model of section 3.4 has two types of exploration. First is the noisy training signal, constantly forcing change in the target angles. Secondly, the network is initially trained with a random policy, while the controller configuration (e.g. the angle representation) assigned to each state is being learned. In this case the network goes through a development period with poor initial performance because this is useful to decouple learning of policies and controller configuration.

In contrast, in section 3.3 exploration happens because pulses or oscillations are produced by the controller in response to the error signals. These are reminiscent jerks and twitches happening at the early stages of motor learning in animals, which for some mammals may happen before birth, and

lead to the foundations of functional proprioception and motor coordination [25]. For the learning rules in section 3.3, using a constantly shifting desired state to encourage exploration would be counterproductive, because sudden shifts in the desired state would reflect as shifts in the error signal, interfering with learning.

Generalizing, training a hierarchical system with the architecture we have suggested would involve starting with the lowest hierarchical levels, and proceeding to the next level once a reasonable performance is achieved. At each level, sensory representation training happens first through exploratory policies, followed by more motivated behaviour.

Overall, our results show how to produce autonomous motor control through a hierarchy of feedback controllers. The learning rules of section 3.1 can readily learn the correlations between sensory features and actuator outputs (which tend to remain stable), whereas more complex, context-dependent control rules can be learned using a second hierarchical level such as that in section 3.4. We expect that through further hierarchical extensions, such as described in 4.2 we will approach truly flexible, animal-like control.

## Supplementary Material

The Appendix and source code for this paper can be obtained from: [https://gitlab.com/sergio.verduzco/public\\_materials](https://gitlab.com/sergio.verduzco/public_materials) in the neurips\_2020 folder.

## References

- [1] R. A. Andersen, G. K. Essick, and R. M. Siegel. Encoding of spatial location by posterior parietal neurons. *Science*, 230(4724):456–458, October 1985. Publisher: American Association for the Advancement of Science Section: Reports.
- [2] Matthew Michael Botvinick. Hierarchical reinforcement learning and decision making. *Current Opinion in Neurobiology*, 22(6):956–962, December 2012.
- [3] E. Bristol. On a new measure of interaction for multivariable process control. *IEEE Transactions on Automatic Control*, 11(1):133–134, January 1966.
- [4] Matteo Carandini and David J. Heeger. Normalization as a canonical neural computation. *Nature Reviews Neuroscience*, 13(1):51–62, January 2012.
- [5] G. Bard Ermentrout and David H. Terman. *Mathematical Foundations of Neuroscience*. Springer Science & Business Media, New York, NY, July 2010. Google-Books-ID: 0fLdzaFgtjcC.
- [6] Michael J. Frank and David Badre. Mechanisms of Hierarchical Reinforcement Learning in Corticostriatal Circuits 1: Computational Analysis. *Cerebral Cortex*, 22(3):509–526, March 2012.
- [7] Dongqi Han, Kenji Doya, and Jun Tani. Self-organization of action hierarchy and compositionality by reinforcement learning with recurrent neural networks. *arXiv:1901.10113 [cs, stat]*, November 2019. arXiv: 1901.10113.
- [8] Bernd Illing, Wulfram Gerstner, and Johanni Brea. Biologically plausible deep learning — But how far can we go with shallow networks? *Neural Networks*, 118:90–101, October 2019.
- [9] Michael I. Jordan and David E. Rumelhart. Forward Models: Supervised Learning with a Distal Teacher. *Cognitive Science*, 16(3):307–354, 1992. \_eprint: [https://onlinelibrary.wiley.com/doi/pdf/10.1207/s15516709cog1603\\_1](https://onlinelibrary.wiley.com/doi/pdf/10.1207/s15516709cog1603_1).
- [10] Christoph Kolodziejewski, Bernd Porr, and Florentin Wörgötter. On the Asymptotic Equivalence Between Differential Hebbian and Temporal Difference Learning. *Neural Computation*, 21(4):1173–1202, November 2008. Publisher: MIT Press.
- [11] Tejas D Kulkarni, Karthik Narasimhan, Ardavan Saeedi, and Josh Tenenbaum. Hierarchical Deep Reinforcement Learning: Integrating Temporal Abstraction and Intrinsic Motivation. In D. D. Lee, M. Sugiyama, U. V. Luxburg, I. Guyon, and R. Garnett, editors, *Advances in Neural Information Processing Systems 29*, pages 3675–3683. Curran Associates, Inc., 2016.

- [12] M Kuperstein. Neural model of adaptive hand-eye coordination for single postures. *Science*, 239(4845):1308–1311, March 1988.
- [13] William Levine, editor. *The Control Systems Handbook: Control System Advanced Methods, Second Edition*. CRC Press, 2011.
- [14] Daniel Liberzon. *Calculus of Variations and Optimal Control Theory: A Concise Introduction*. Princeton University Press, 2012. Google-Books-ID: mhklgjmACRUC.
- [15] Eve Marder and Dirk Bucher. Central pattern generators and the control of rhythmic movements. *Current Biology*, 11(23):R986–R996, November 2001.
- [16] Josh Merel, Matthew Botvinick, and Greg Wayne. Hierarchical motor control in mammals and machines. *Nature Communications*, 10(1):1–12, December 2019.
- [17] Hiroyuki Miyamoto, Mitsuo Kawato, Tohru Setoyama, and Ryoji Suzuki. Feedback-error-learning neural network for trajectory control of a robotic manipulator. *Neural Networks*, 1(3):251–265, January 1988.
- [18] Volodymyr Mnih, Koray Kavukcuoglu, David Silver, Andrei A. Rusu, Joel Veness, Marc G. Bellemare, Alex Graves, Martin Riedmiller, Andreas K. Fidjeland, Georg Ostrovski, Stig Petersen, Charles Beattie, Amir Sadik, Ioannis Antonoglou, Helen King, Dharmashan Kumar, Daan Wierstra, Shane Legg, and Demis Hassabis. Human-level control through deep reinforcement learning. *Nature*, 518(7540):529–533, February 2015.
- [19] Kenji Morita, Jenia Jitsev, and Abigail Morrison. Corticostriatal circuit mechanisms of value-based action selection: Implementation of reinforcement learning algorithms and beyond. *Behavioural Brain Research*, 311:110–121, September 2016.
- [20] D. A. Novikov. *Cybernetics: From Past to Future*. Springer, December 2015. Google-Books-ID: LbQvCwAAQBAJ.
- [21] Yu-Cheng Pei, Steven S. Hsiao, James C. Craig, and Sliman J. Bensmaia. Shape Invariant Coding of Motion Direction in Somatosensory Cortex. *PLoS Biology*, 8(2), February 2010.
- [22] Bernd Porr and Florentin Wörgötter. Strongly Improved Stability and Faster Convergence of Temporal Sequence Learning by Using Input Correlations Only. *Neural Computation*, 18(6):1380–1412, April 2006.
- [23] William T. Powers. *Behavior: The Control of Perception (2nd ed. rev. & exp.)*, volume xiv. Benchmark Press, New Canaan, CT, US, 2005.
- [24] Daniel Rasmussen, Aaron Voelker, and Chris Eliasmith. A neural model of hierarchical reinforcement learning. *PLOS ONE*, 12(7):e0180234, July 2017.
- [25] Scott R. Robinson, Gale A. Kleven, and Michele R. Brumley. Prenatal Development of Interlimb Motor Learning in the Rat Fetus. *Infancy : the official journal of the International Society on Infant Studies*, 13(3):204–228, May 2008.
- [26] Uri Rokni. Neural Networks for Control. *Encyclopedia of Neuroscience*, pages 2592–2596, 2009. Publisher: Springer, Berlin, Heidelberg.
- [27] Tom Schaul, Daniel Horgan, Karol Gregor, and David Silver. Universal Value Function Approximators. pages 1312–1320, June 2015. ISSN: 1938-7228 Section: Machine Learning.
- [28] Wolfram Schultz, Peter Dayan, and P. Read Montague. A Neural Substrate of Prediction and Reward. *Science*, 275(5306):1593–1599, March 1997.
- [29] David Silver, Julian Schrittwieser, Karen Simonyan, Ioannis Antonoglou, Aja Huang, Arthur Guez, Thomas Hubert, Lucas Baker, Matthew Lai, Adrian Bolton, Yutian Chen, Timothy Lillicrap, Fan Hui, Laurent Sifre, George van den Driessche, Thore Graepel, and Demis Hassabis. Mastering the game of Go without human knowledge. *Nature*, 550(7676):354–359, October 2017.
- [30] Eduardo D. Sontag. *Mathematical Control Theory: Deterministic Finite Dimensional Systems*. Springer Science & Business Media, November 2013. Google-Books-ID: f9XiBwAAQBAJ.
- [31] Richard S. Sutton and Andrew G. Barto. *Reinforcement Learning: An Introduction*. MIT Press, November 2018. Google-Books-ID: sWV0DwAAQBAJ.
- [32] Sergio Verduzco-Flores and Erik De Schutter. Draculab: A Python Simulator for Firing Rate Neural Networks With Delayed Adaptive Connections. *Frontiers in Neuroinformatics*, 13, 2019.